4. Injection Molding

Preface

This chapter is focused on the second and third objectives of this research. In particular, the effect of fiber draw ratio on the final mechanical properties is examined. Also, the effect of matrix viscosity on mechanical properties is studied and the issue of how dilution affects mechanical properties is investigated. This chapter is organized as a manuscript for future publication.

Injection Molding of PET Reinforced with Pregenerated TLCP Micro-Fibrils

M.A. McLeod and D.G. Baird

Department of Chemical Engineering
Virginia Polytechnic Institute and State University
Blacksburg, VA 24061-0211

(ABSTRACT)

This work was concerned with the injection molding of composite materials based on poly(ethylene terephthalate) (PET) reinforced with pregenerated thermotropic liquid crystalline polymer (TLCP) fibrils, where the TLCP had a higher melting temperature than PET. Three TLCPs and one TLCP/TLCP blend were evaluated for their potential use in the pregenerated microcomposite processing scheme. From this evaluation, an apparently amorphous TLCP manufactured by DuPont, HX1000, was determined to be the best candidate. Using this TLCP, pregenerated microcomposites were made using a two step process. First, a novel dual extrusion process was used to produce composite strands of PET/TLCP containing nearly continuous TLCP fibrils. Second, these composite strands were subsequently chopped into pellets and injection molded below the melt processing temperature of the TLCP but above that of the matrix. This allowed the high modulus TLCP fibrils generated in the spinning step to be retained in the final injection molded sample. TLCP concentration in the composite strands and composite strand draw ratio were varied to determine their effects on mechanical properties. It was shown that the best mechanical properties were produced using high draw ratio strands containing 50 weight percent HX1000, which were diluted with a low viscosity injection molding grade of PET to the desired loading level. These pregenerated microcomposites possessed machine direction moduli which were always greater than 70% of the theoretically expected values. Although the machine direction properties of the injection molded microcomposites were about 35% to 50% lower than those of glass-filled PET when compared at the same weight percent reinforcement, their surfaces were significantly smoother than those of the glass-filled PET.

4.1 Introduction

The use of thermotropic liquid crystalline polymers (TLCPs) to reinforce commodity thermoplastics has attracted considerable interest since the mid to late 1980's [1 - 5]. One reason for this interest has been due to the fact that when blends of a thermoplastic and a TLCP are subjected to extensional deformation, the TLCP phase is deformed into fibrils. These TLCP fibrils are found to provide mechanical reinforcement to the matrix, producing light weight, wholly thermoplastic composites. Because the reinforcing fibrils are formed during the melt processing step, Kiss [3] called the resulting materials *in situ* composites.

There are several reasons that TLCPs are potentially viable alternatives to traditional reinforcing materials like glass fiber. One significant reason is their combination of low density and high mechanical properties. It has been shown that neat TLCPs can possess moduli of up to 100 GPa and strengths of 1 GPa and greater when they are highly oriented, while having densities of only around 1.4 g/cm^3 [6- 8]. These properties are competitive with other forms of reinforcement, such as glass fiber, which has a tensile modulus of 69 to 83 GPa, a tensile strength from 1.72 to over 2.07 GPa, and a density of 2.52 to 2.61 g/cm^3 [9 - 12]. Therefore, if the full reinforcing potential of the TLCP is realized, it would be possible to produce wholly thermoplastic composites which would have mechanical properties matching or exceeding those obtained of glass and aramid fibers are used as the reinforcement. Other important reasons cited for using TLCPs as reinforcement rather than glass fiber are: 1) the melt is easier to process, 2) there is less wear on the processing equipment, 3) the ability to use compatibilization to provide interfacial adhesion between the two phases, and 4) their recycling potential [13]. Therefore, TLCPs possess several key features which make them a possible alternative to more conventional reinforcing materials.

Despite the potential of TLCPs as reinforcing materials, it has been shown that injection molded in situ composites typically have not achieved theoretically expected levels of reinforcement. For example, Datta et al. [14] produced in situ composites using polypropylene (PP) as the matrix, maleated polypropylene as a component to promote adhesion, and a polyesteramide, Vectra B950, as the TLCP. After injection molding, test samples were cut from the composite plaques in both the machine and transverse directions so mechanical property measurements could be made. At a loading of 20 wt% Vectra B950, the machine direction modulus was 3.209 GPa and the transverse direction modulus was 1.937 GPa. Although these values were significantly higher than the 1.384 GPa modulus of the neat PP, it was still well below theoretical expectations, based on the Halpin-Tsai equation [15] and properties for the neat TLCP. In particular, using a tensile modulus of 75 GPa for Vectra B950 yielded a theoretical modulus of 5.27 GPa for a planar isotropic plaque [16]. The reason that the experimental properties of these composites were lower than the predicted values was because the flow kinematics during mold filling did not subject all of the TLCP to strong extensional deformation, creating a skin-core morphology with unoriented TLCP in the core [17].

Another significant drawback of injection molded in situ composites is the planar anisotropic distribution of mechanical properties, with high flow direction properties and low transverse direction properties [13, 18]. Bafna and coworkers [19] showed this mechanical anisotropy by using a film-gated mold to produce composites containing polyetherimide (PEI) as the matrix and HX1000, a polymer believed to be composed of hydroquinone, 4-hydroxybenzoic acid, terephthalic acid, and substituted hydroquinones, as the TLCP. At a loading of 50 wt% HX1000, over a 4 to 1 ratio of mechanical anisotropy was observed for the flexural modulus. In particular, the machine direction modulus was 12.92 GPa while the transverse modulus was only 3.20 GPa. It should be noted that PEI has a modulus of 3.0 GPa, demonstrating that the TLCP did not reinforce the transverse direction significantly.

A final problem with in situ composites is that mechanical properties are strongly dependent on injection molding conditions, such as mold thickness, fill rate, mold temperature, and melt temperature [20, 21, 22]. For example, O'Donnell [20, 22] injection molded plaques 1.0 mm, 1.5 mm, and 2.3 mm thick composed of PP/maleated PP/Vectra B950 (63/7/30 wt%). The mold was kept at 50°C and the injection speed was varied. Comparing machine direction results on the mechanical properties of plaques injection molded at a volumetric flow rate of about 14.5 cm^3, the 1.5 mm thick plaque had the highest flexural modulus (5.10 GPa) and strength (60.5 MPa). This contrasts sharply with the properties from the other two molds. Plaques from the 1.0 mm mold had a modulus of 3.71 GPa and a strength of 54.2 MPa, while 2.3 mm thick plaques possessed values of just 4.61 GPa and 54.5 MPa. These results demonstrated that the ability to maximize mechanical properties can be appreciably limited by the processing variables.

In order to surmount many of the problems with in situ composites, investigations have been conducted where injection molded composites were produced in two steps rather than one [23 - 26]. First, the TLCP/matrix melt was spun into composite strands, orienting the TLCP molecules. Second, the strands were chopped into pellets and injection molded below the melting temperature of the TLCP to form a composite part. This two step process creates a wholly thermoplastic composite with the pregenerated TLCP fibrils stiffening the matrix, much in the same way as glass fiber is used to stiffen thermoplastics. Specifically, the fiber spinning step serves to orient all of the TLCP phase, while the injection molding step serves to form a part with the reinforcement distributed in both the machine and transverse directions. Because the TLCP fibrils were formed prior to the injection molding step and had diameters of the order of a micron, Handlos and Baird [25] called the resulting materials *pregenerated microcomposites*.

Using pelletized composite strands generated with a patented dual extruder system [27, 28], Handlos and Baird [25] injection molded pregenerated microcomposite plaques containing 10 wt%, 20 wt%, and 30 wt% TLCP and demonstrated that the problem of planar anisotropy was significantly reduced. In this study, the matrix was PP while two different TLCPs were used as the reinforcing phase. The first was Vectra A950, a copolyester of 4-hydroxybenzoic acid (HBA) and hydroxynaphthoic acid (HNA) (73/27 mol%) produced by Hoechst Celanese, while the second was HX 6000, a polyester believed to be composed of hydroquinone, 4-hydroxybenzoic acid, terephthalic acid, and substituted hydroquinones produced by DuPont. Also, it should be noted that the PP contained 10 wt% maleated PP (MAP) to promote adhesion between the matrix and the TLCP. For PP (10 wt% MAP)/Vectra A950 (80/20 wt%) pregenerated microcomposites, the machine direction tensile modulus was 2.31 GPa and the transverse direction tensile modulus was 2.18 GPa, making the ratio of the two moduli 1.06. Similar results were observed with PP(10 wt% MAP)/HX6000 (80/20 wt%) pregenerated microcomposites, with the machine direction modulus being 3.23 GPa, the transverse direction modulus being 2.44 GPa, and the ratio of the two moduli being 1.31. This degree of anisotropy compared favorably with PP containing 20 wt% glass fiber, which showed a machine to transverse direction moduli ratio of 1.31. This suggested that the TLCP fibrils and the glass fibers were distributed similarly in the plaques.

On the other hand, the pregenerated microcomposites did not reach their theoretically predicted levels of stiffness. Handlos and Baird [25] reported that the PP(10 wt% MAP)/HX6000 (70/30 wt%) pregenerated microcomposites had a machine direction modulus of 3.98 GPa and a transverse direction modulus of 2.91 GPa. Although these values were significantly greater than the modulus of 1.0 GPa of the neat PP, they were below the value of 5.20 GPa which was predicted using composite theory. Three reasons cited as possible causes for the discrepancy between the experimental and theoretical moduli were 1) molecular relaxation due to the TLCP becoming too hot, 2) agglomeration of the TLCP fibrils, and 3) loss of aspect ratio due to fiber breakage as a result of the shear stresses in the injection molding step. Still, the morphology showed that fibrils were present throughout the thickness of the specimens. Hence, if the fibrils were not damaged in the injection molding step, it should have been possible to reach the maximum predicted modulus.

There are two purposes to this paper. The first is to show the criteria needed for a TLCP to be an acceptable candidate for the pregenerated microcomposite process. Namely, the thermal transitions of several TLCPs will be discussed along with their dynamic mechanical properties as they are heated and their complex viscosities as they are cooled relative to those of the matrix PET. The second purpose is to show how the matrix viscosity and strand loading level affect the properties of the injection molded pregenerated microcomposites, with the goal of attempting to overcome the problems in maintaining mechanical properties reported by Handlos and coworkers [24, 25, 26]. Additionally, the tensile, flexural, dynamic mechanical, and surface roughness properties of these materials will be compared to the properties of neat PET and glass filled PET.

4.2 Experimental

4.2.1 Materials

Three TLCPs produced by DuPont were used in this study: 1) HX1000, 2) HX6000, and 3) HX8000. HX1000 is an apparently amorphous TLCP (at least there is no discernible melting point) with a glass transition temperature of approximately 160°C and a density of 1.25 g/cm^3. For processing, it typically has to be taken to a melt temperature of at least 310°C. HX6000 is a semicrystalline TLCP with no discernible glass transition temperature, two melting temperatures (one at 275.5°C and the second at 331.9°C), and a density of 1.38 g/cm^3. A melt temperature of at least 350°C is usually needed for processing. HX8000 is a semicrystalline TLCP with a glass transition temperature of 110°C, two melting temperatures (one at 228.9°C and the second at 271.8°C), and a density of 1.38 g/cm^3. To process this TLCP, a melt temperature of at least 290°C is usually required. It is believed these TLCPs are composed of unspecified ratios of terephthalic acid, 4-hydroxybenzoic acid, hydroquinone, and hydroquinone derivatives [7, 29- 37]. HX1000 is believed to contain bulky substituents on the main chain which make it amorphous [7, 30].

A high viscosity grade of poly(ethylene terephthalate) (PET) was used as the matrix in the spinning step (PT 7067, DuPont). It has a glass transition temperature of 84°C, a melting temperature of 255°C, an inherent viscosity of 0.98, and a density of 1.33 g/cm^3 [38]. In the injection molding step, the chopped composite strands were dry blended with pellets of Rynite, an experimental, low viscosity injection molding grade of PET produced by DuPont which contains a nucleating agent to promote crystallization. It has a density of 1.36 g/cm^3, a glass transition temperature of around 88°C, and a melting temperature of 257°C. Rynite 530, a PET manufactured by DuPont that contains 30 wt% glass reinforcement, was also injection molded. All polymers were dried in a vacuum oven set at 110°C for at least 24 hours before processing and their mechanical properties are presented in Table 4.1.

4.2.2 Composite Strand Processing

Composite strands of PT 7067 and HX1000 were generated using a patented dual extrusion process, which has been extensively described elsewhere [27, 28, 39]. Strands were spun with two loadings of TLCP, either 20 wt% TLCP or 50 wt% TLCP. The equipment consisted of two Killion KL-100 extruders having a screw diameter of one inch and a L/D = 24. Regardless of the loading of TLCP in the composite strands, the HX1000 was processed in one extruder with the melt conveying zone set at 310°C to 330°C while the PT 7067 was plasticated in the second extruder with the melt conveying

Table 4.1: The Mechanical Properties of Injection Molded Neat and Glass Fiber Filled PET

	Tensile Properties		Flexural Properties	
PT 7067				
	Machine Direction	Transverse Direction	Machine Direction	Transverse Direction
Modulus (GPa)	2.176 (0.067)	2.225 (0.056)	2.501 (0.092)	1.951 (0.157)
Strength (MPa)	47.87 (2.063)	50.31 (1.089)	70.16 (2.228)	61.27 (2.627)
% Elongation	3.384 (0.397)	3.655 (0.169)		
Rynite				
	Machine Direction	Transverse Direction	Machine Direction	Transverse Direction
Modulus (GPa)	2.424 (0.217)	2.585 (0.246)	2.763 (0.194)	2.579 (0.085)
Strength (MPa)	49.40 (0.883)	42.85 (6.852)	69.04 (0.311)	67.45 (2.784)
% Elongation	2.760 (0.137)	1.924 (0.411)		
10 wt% Glass Fiber Filled PET				
	Machine Direction	Transverse Direction	Machine Direction	Transverse Direction
Modulus (GPa)	3.656 (0.276)	3.476 (0.171)	4.149 (0.334)	3.492 (0.325)
Strength (MPa)	62.41 (3.999)	58.10 (2.568)	100.81 (5.215)	90.26 (5.299)
% Elongation	2.321 (0.580)	2.253 (0.634)		
Toughness (MPa)	0.979 (0.166)	0.914 (0.149)		
20 wt% Glass Fiber Filled PET				
	Machine Direction	Transverse Direction	Machine Direction	Transverse Direction
Modulus (GPa)	6.269 (1.011)	4.042 (0.287)	5.773 (0.261)	4.085 (0.232)
Strength (MPa)	84.90 (4.510)	62.73 (3.245)	134.88 (6.023)	99.24 (6.386)
% Elongation	2.253 (0.333)	2.234 (0.337)		
Toughness (MPa)	1.283 (0.293)	0.929 (0.202)		
30 wt% Glass Fiber Filled PET				
	Machine Direction	Transverse Direction	Machine Direction	Transverse Direction
Modulus (GPa)	9.209 (0.635)	4.711 (0.551)	10.045 (0.349)	4.999 (0.327)
Strength (MPa)	117.8 (5.118)	59.12 (4.268)	205.43 (4.184)	98.16 (9.178)
% Elongation	1.722 (0.090)	1.368 (0.178)		
Toughness (MPa)	1.458 (0.213)	0.843 (0.166)		

Note: Standard deviations given in parentheses.

zone set at 275°C to 285°C. The mass flow rate of the TLCP was accurately metered by using a Zenith gear pump (Model HD-556, 1.725 cm^3/rev.), with the strand composition determined from the total mass flow rate of the blend and the controlled mass flow rate of the TLCP. After passing through the gear pump, the TLCP stream was cooled to 300°C before being introduced into the PT 7067 using a tee connecting the two extruders. Immediately following the tee, the HX1000/PT 7067 blend was passed through a mixing head containing three helical elements and a Koch static mixer with four elements to further divide the TLCP into smaller continuous streams. The melt was then passed through a capillary die (L/D<1, exit diameter = 1.8 mm), drawn to orient the TLCP, quenched in a water bath, and collected on a take-up roll. The strand draw ratios were calculated as the die exit diameter squared divided by the square of the measured strand diameter. It should be noted that the drawing was performed using a vertical drawing chimney that was approximately 4 meters long. The chimney insulated the spinning line from air currents in the building, helping keep the spinning process stable and assisting in reaching high strand draw ratios.

4.2.3 Injection Molding

The injection molder used in this work was an Arburg Allrounder Model 221-55-250. It has a screw with a 22 mm diameter, a check ring non-return valve, and an insulated nozzle tip with an exit diameter of 2 mm. The polymer was injected into a film-gated mold having dimensions of 75 mm by 80 mm by 1.60 mm. The injection pressure (5 MPa), holding pressure (10 MPa), mold temperature (110°C), and screw speed (200 rpm) were held constant. The cooling time in the mold for the pregenerated microcomposites was 8 seconds.

Pregenerated microcomposites were injection molded with loading levels of 10, 20, and 30 wt% TLCP. Strands containing 20 wt% TLCP were simply chopped to a length of about 3 mm and injection molded. Meanwhile, strands containing 50 wt% TLCP were chopped to a length of about 3 mm and then dry blended with Rynite to reduce the TLCP concentration to 10, 20, and 30 wt%. Once dry blended with pellets of Rynite, they were injection molded to produce the pregenerated microcomposites.

The barrel temperatures were varied according to the material being injection molded, with the heating zones progressing from the solids conveying zone (zone 1) to the nozzle (zone 4). The pregenerated microcomposites were injection molded with the barrel temperatures set at: zone 1 = 245°C, zone 2 = 250°C, zone 3 = 250°C, and zone 4 = 250°C. These were the lowest temperature settings that could be used without having solidification in the nozzle tip. Rynite, PT 7067, and glass fiber filled PET were injection molded using the following barrel temperatures: zone 1 = 250°C, zone 2 = 270°C, zone 3 = 280°C, and zone 4 = 280°C. Neat plaques of HX6000 and HX6000/HX8000 (50/50 wt%) were injection molded with barrel temperatures of: zone 1 = 310°C, zone 2 =

350°C, zone 3 = 360°C, and zone 4 = 310°C, while zones 2 and 3 were lowered to 330°C to injection mold plaques of HX1000 and HX8000.

4.2.4 Mechanical Properties

All of the tensile properties of the individual composite strands were measured using an Instron Mechanical Tester (model 4204) equipped with a 1 kN load cell. The gage lengths were approximately 250 mm, with the fiber ends wrapped with masking tape to provide uniform gripping of the strands. The crosshead speed was set at 1.27 mm/min.

The tensile and flexural properties of the injection molded composites and compression molded strands were also measured using an Instron Mechanical Tester (model 4204), with the tensile tests performed using a 5 kN load cell and the flexural tests performed using a 1 kN load cell. To perform the tests, specimens that measured approximately 75 mm long by 12.5 mm wide were cut from the plaques. These specimens were then carefully sanded to smooth the cut surfaces. ASTM standard B 638-87B was followed for the tensile testing of these samples, with the crosshead speed kept at 1.27 mm/min and the strain measured using an extensiometer (Instron model 2630-25). For the three-point bending tests, the ASTM standard D 790M 86 was adhered to. Note that for all of the tensile and flexural test results, the reported values were an average of at least five samples. Strength, % elongation, and toughness values were all determined based on yield rather than at fracture, if the sample yielded before breaking.

4.2.5 Morphology

The morphology of the strands and plaques was examined using a Stereoscan S200 scanning electron microscope with an accelerating voltage of 15 kV. To prepare the samples, they were immersed in liquid nitrogen for at least two minutes, then fractured. They were subsequently attached to mounting stubs and coated with a layer of gold using an SPI sputter coater to enhance conductivity.

4.2.6 Dynamic Mechanical Thermal Analysis

The complex viscosities ($|\eta^*|$) of the polymers were measured using a Rheometrics RMS-800 with 25 mm diameter parallel plate tooling and test specimens cut from injection molded plaques. A gap distance of 1.0 mm was used for all of the tests conducted on the TLCPs. The temperature was held constant for three minutes before starting each test to establish thermal equilibrium between the tooling and the melt. Also, a strain of 5% was always used and the samples were exposed to a continuous nitrogen atmosphere.

For the dynamic mechanical thermal analysis, machine direction strips were cut from injection molded plaques and tested in torsion using a Rheometrics RMS-800. Each test was performed in air with a heating rate of 2.5°C/min., an angular frequency (ω) of 10 rad/sec, and a strain of 0.1%. The starting temperature used was just above ambient, between 30°C to 50°C. To expose the samples to 260°C for one minute, the RMS oven was heated to 260°C, then the sample was suspended in the heated oven with a thermocouple taped to the specimen surface. It took one and a half minutes for each specimen to reach 260°C, after which it was kept in the oven for an additional minute, then removed and quenched in an ice bath.

4.2.7 Surface Roughness

The surface roughness values of the glass-fiber filled PET and the pregenerated microcomposites were determined using a Tencar Alpha-Step 500 surface profiler. The measurements were made using a stylus with a 12.5 μm tip radius, a scan speed of 100 μm/second, and a scan length of 500 μm. The reported values are averages of ten measurements.

4.3 Results and Discussion

4.3.1 Evaluation of the TLCPs

Before producing the PET-based pregenerated microcomposites, each TLCP needed to be evaluated to determine if they possessed the characteristics required for this processing scheme. First, the TLCP needed to be processable below 300°C in order to combine it with PET which degrades at temperatures above 300°C. Second, it had to retain its mechanical properties after subjecting it to temperatures at least as high as 260°C.

To determine how the complex viscosities of the TLCPs changed with cooling, each TLCP was heated to the maximum temperature the TLCP would be exposed to during processing in the dual extruder system, then cooled at a rate of 2.3°C/min (± 0.1°C/min). The maximum temperature of 330°C was used to HX1000 and HX8000, to insure that no high melting crystallites were present in the melt. High melting crystallites have been observed with other TLCPs [40, 41] and can prevent mechanical properties from being maximized [42, 43, 44]. The reason that both HX6000 and HX6000/HX8000 (50/50 wt%) were taken to 360°C was because HX6000 is typically processed at 350°C to 360°C. In particular, to produce a HX6000/HX8000 (50/50 wt%) blend, it was necessary to heat the melt to around 360°C.

The complex viscosities of the TLCPs as a function of temperature are presented in Figure 4.1. Examining the results for each material showed that not all of the TLCPs could be cooled to 300°C without solidifying. As HX6000 was cooled to below 330°C, its complex viscosity began to rise dramatically, reaching nearly 10,000 Pa·s at 317°C. Meanwhile, both HX8000 and HX6000/HX8000 (50/50 wt%) solidified at temperatures well under 300°C. Also, it was clear that HX1000 remained deformable as it was cooled below 300°C. Considering this data, it was clear that HX6000 could be eliminated as a candidate for processing with PET because the HX6000 could not be kept deformable without exceeding the degradation temperature of PET.

Before deciding that HX1000, HX8000, and HX6000/HX8000 (50/50 wt%) could be used to produce composite strands with PET, one additional criterion had to be met. To produce composite strands, the viscosity of the TLCP needed to be lower than or similar to that of the PET in order to effectively deform the TLCP [13, 18, 45]. Comparing the complex viscosities of these three TLCPs to that of PT 7067 showed that this requirement was met in each case. The viscosity of HX6000/HX8000 (50/50 wt%) exceeded that of PT 7067 only for temperatures under 280°C, while HX8000 remained less viscous until the temperature reached about 252°C. Additionally, the viscosity of HX1000 remained below that of PT 7067 for the entire cooling test. From these results it can be stated that each of these TLCPs met the rheological requirements needed for the dual extruder processing scheme.

Next, to evaluate the TLCPs for the pregenerated microcomposite process, dynamic mechanical thermal analysis was performed on machine direction strips cut from injection molded plaques of the neat materials (Figure 4.2 and Figure 4.3). This was done to: 1) determine how the storage modulus of each TLCP changed with temperature, especially just above the melting temperatures of PT 7067 and Rynite, and 2) determine how brief exposure to 260°C would affect the storage moduli of the TLCPs. It was found that each TLCP retained its stiffness after being exposed to 260°C for one minute, with the storage moduli matching those of the samples which had not been heated to 260°C (Figure 4.2 and Figure 4.3). This result indicated that the TLCPs should not be expected to lose their mechanical properties due to brief exposure to 260°C. However, it should be noted that the three remaining candidates, HX1000, HX6000/HX8000 (50/50 wt%), and HX8000, all showed that they had softened appreciably when taken to 260°C.

In the final evaluation of the TLCPs, they were heated at a rate of 20.0°C/min using differential scanning calorimetry (DSC) to determine their thermal transitions. In particular, it had to be determined if HX1000, HX8000, or HX6000/HX8000 (50/50 wt%) exhibited any secondary melting endotherms, which, if they existed, would need to be compared to the melting temperatures of Rynite and PT 7067. For HX6000/HX8000 (50/50 wt%), the results were not encouraging for its use in PET-based pregenerated microcomposites. In addition to exhibiting a glass transition temperature at 110°C, it had

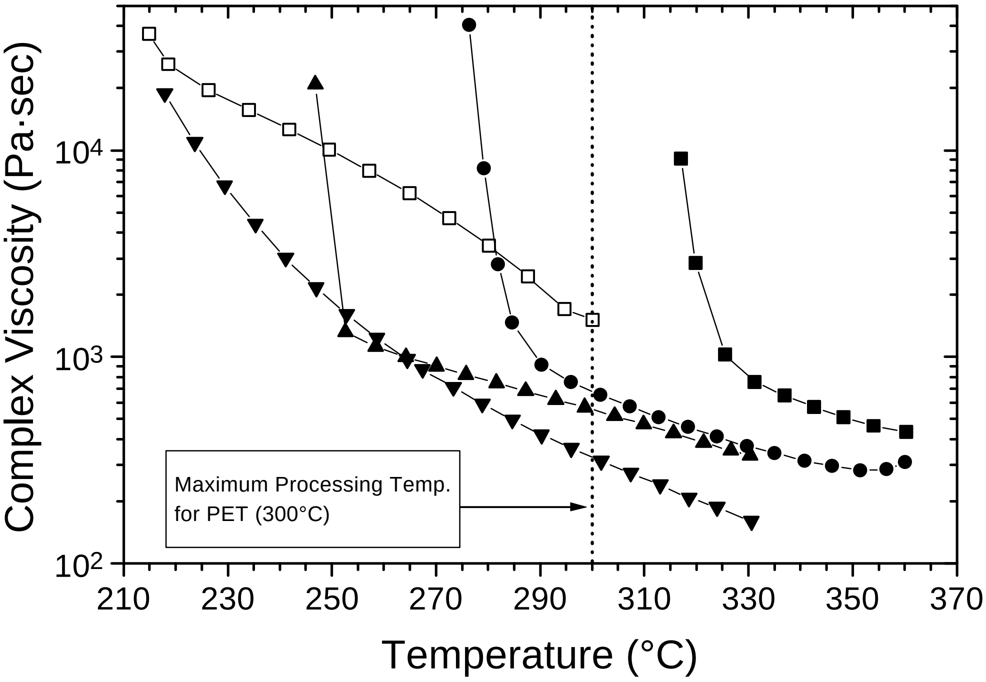

Figure 4.1: Complex viscosity (|η*|) as a function of temperature for polymers cooled at a rate of 2.3°C/min. (□) = PT 7067, (■) = HX6000, (●) = HX6000/HX8000 (50/50 wt%), (▲) = HX8000, and (▼) = HX1000.

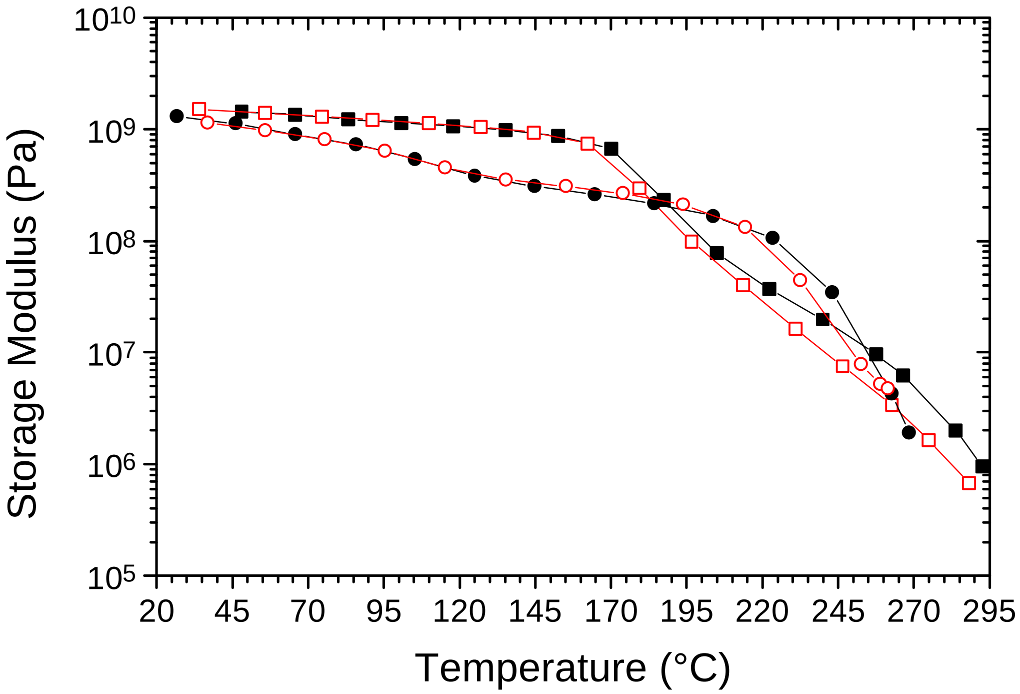

Figure 4.2: The storage modulus (G') as a function of temperature for TLCPs heated at a rate of 2.5°C/min. (■) = HX1000, (●) = HX8000, (□) = HX1000 exposed to 260°C for 1 minute, and (○) = HX8000 exposed to 260°C for 1 minute.

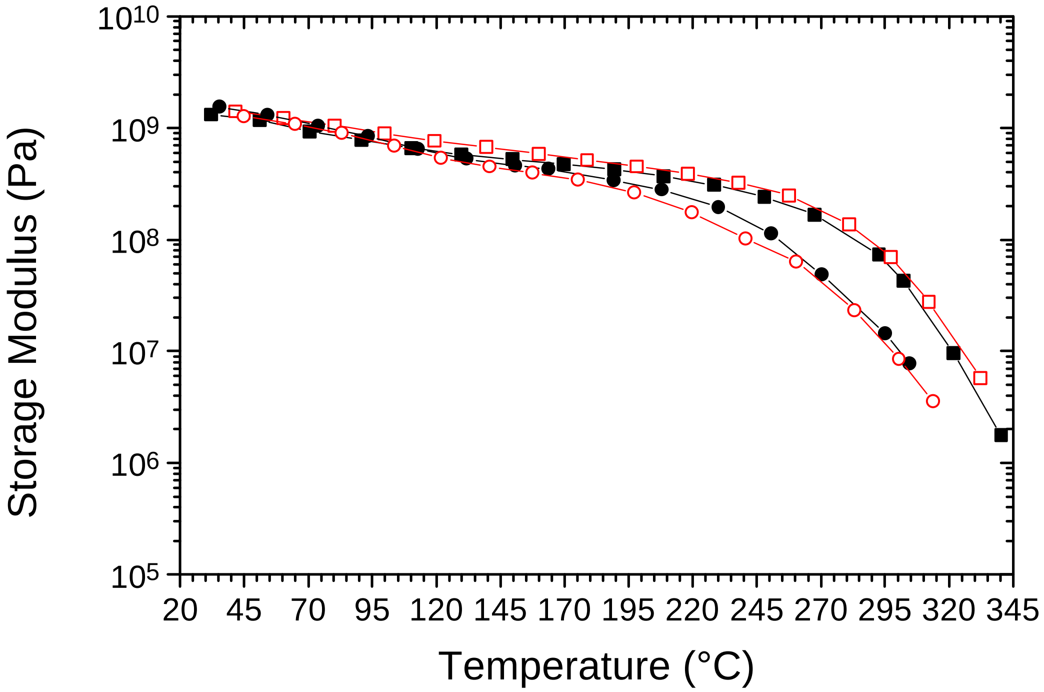

Figure 4.3: The storage modulus (G') as a function of temperature for TLCPs heated at a rate of 2.5°C/min. (■) = HX6000, (●) = HX6000/HX8000 (50/50 wt%), (□) = HX6000 exposed to 260°C for 1 minute, and (○) = HX6000/HX8000 (50/50 wt%) exposed to 260°C for 1 minute.

two melting endotherms, a broad peak at 249°C as well as a second sharper peak at 308°C. HX8000 revealed similar behavior, with a glass transition temperature around 110°C, a broad melting endotherm at 229°C and a second melting endotherm at 271.8°C. Because of both of these TLCP would have to be taken to a temperature approximately 150°C higher than their glass transition temperatures as well as above their first melting peaks, these two TLCPs were dismissed as candidates for the pregenerated microcomposite process. It should be noted that further testing of HX6000/HX8000/PT 7067 composite strands confirmed that properties would not be retained [49]. Meanwhile, for HX1000, the results were more encouraging. The DSC data showed a glass transition temperature at 160°C, which was nearly the same temperature where the storage modulus was shown to begin to decline, as well as no melting endotherms. Therefore, in using HX1000 to produce PET-based pregenerated microcomposites, it would have to be taken to a temperature roughly 100°C above its glass transition temperature. Although this temperature difference is high, it was better than either HX8000 or HX6000/HX8000 (50/50 wt%) showed, so HX1000 was concluded to be the best candidate for the pregenerated microcomposite process.

4.3.2 Tensile Properties of Neat Materials

Having decided to use HX1000 as the reinforcing phase for the pregenerated microcomposites, the mechanical properties of HX1000 and the matrix resins were measured. This entailed spinning the TLCP into strands at various draw ratios to determine how their mechanical properties changed with increased draw. Also, the strand properties were compared with those of the matrix resins, focusing on the difference in stiffness between the TLCP strands and the matrix resins. The draw ratios were calculated using the conservation of mass, dividing the die exit diameter squared by the fiber diameter squared.

The tensile testing of the neat HX1000 strands showed that higher draw ratios yielded higher moduli. Spinning the HX1000 melt into strands resulted in the modulus increasing for draw ratios up to 50, at which point it leveled off at a value of around 50 GPa (Figure 4.4). This behavior closely matches the results reported by Sabol et al. [24], where the tensile modulus was found to be around 53.3 GPa for strands with draw ratios greater than 50.

The effect of draw ratio on tensile strength was also investigated for the HX1000 strands. The results demonstrated that no discernible relationship existed between strand draw ratio and the tensile strength of HX1000. Irrespective of the draw ratio, the HX1000 strands had a tensile strength of 271.4 MPa (± 86.6 MPa) (standard deviations are shown in parentheses). However, this result may be due to the brittleness of the strands. Experimentally, this led to problems such as the fibers breaking in the grips, which in turn made the standard deviation very large. Thus, the lack of an increase in

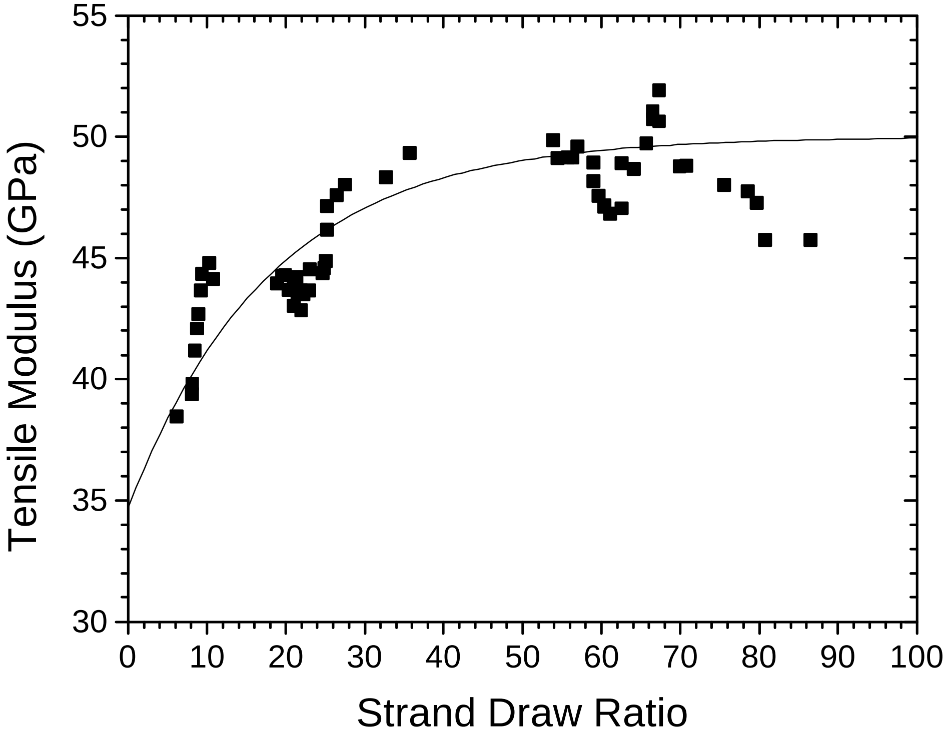

Figure 4.4: Tensile modulus versus draw ratio for HX1000 strands.

strength with increasing draw ratio may be an artifact of the inability to make more accurate measurements.

For the sake of comparison to the properties of the neat HX1000 and the composite strands, the tensile modulus and strength were found for both PT 7067 and Rynite. Also, because PT 7067 was going to be both spun and injection molded in the pregenerated microcomposite process, the mechanical properties were measured for both spun strands and injection molded plaques. Draw ratio was found to have no affect on the properties of melt spun PT 7067. For example, at a draw ratio of 190 (± 36), the PT 7067 fibers had a stiffness of 2.24 GPa (± 0.15 GPa) and a tensile strength of 51.4 MPa (± 5.0 MPa). Within the standard deviations of the measurements this is the same as the injection molded PT 7067, which had a modulus of 2.18 GPa (± 0.07 GPa) and a strength of 47.9 MPa (± 2.1 MPa). Meanwhile, the modulus of Rynite, the injection molding grade PET, was slightly higher at 2.42 GPa (± 0.22 GPa).

4.3.3 Tensile Properties of the Composite Strands

The moduli of the composite strands of HX1000/PT 7067 (50/50 wt%) were measured to determine how they changed with draw ratio. For the HX1000/PT 7067 strands, it was found that the modulus increased up to draw ratios of 40 to 50, matching the relationship between draw ratio and modulus found for neat HX1000. Once the draw ratio reached 40 to 50, additionally drawing did not change the composite strand stiffness and it leveled off at around 25 GPa. One point that needs to be remarked upon was the large standard deviations observed in some of the measurements. The error in draw ratio was due to two factors: 1) the measurements on the strand diameters were accurate to only the hundredth decimal place (± 0.01 mm) and 2) all of the strands typically had fluctuations in diameter of a few hundredths of a millimeter. Because the highest draw ratio strands had diameters of only 0.18 mm to 0.25 mm, the limited accuracy in the diameter measurements and the fluctuations in diameter both contributed to the large standard deviations. For the large standard deviations in the modulus, occasionally a strand exhibited low stiffness. Although this was likely due to the composite strand being slightly damaged, such as being lightly crimped at one location along the length of the strand, these data were not discarded because the source of the error was not identified with certainty.

To confirm that the maximum reinforcing potential was being reached in the composite strands, the rule of mixtures [46] was used to determine the theoretically expected moduli, which were then compared to the experimental data. For the HX1000/PT 7067 composite strands, the rule of mixtures calculations were in agreement with the experimental data, with the modulus achieving a maximum value of approximately 25 GPa (Figure 4.5). From this, it can be concluded that the HX1000 fibrils provided their full reinforcing ability.

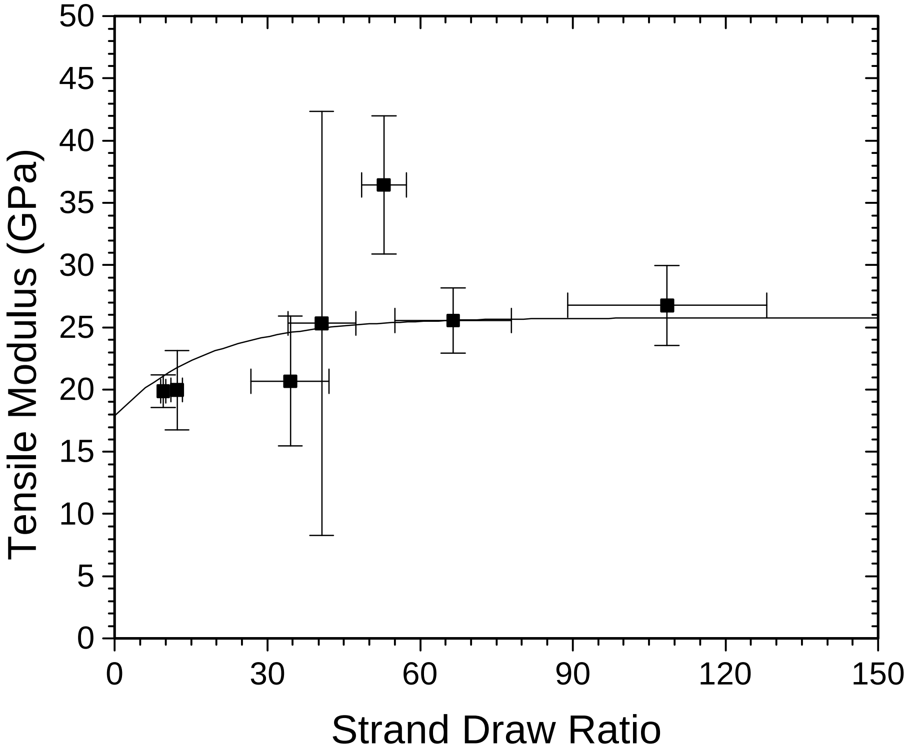

Figure 4.5: Tensile modulus versus draw ratio for HX1000/PT 7067 (50/50 wt%) strands. Experimental data = (■) and rule of mixtures predictions = (__).

The effect that draw ratio had on the tensile strength of the composite strands was also determined, as shown in Figure 4.6. For the HX1000/PT 7067 (50/50 wt%) composite strands, the highest strengths were achieved at the highest draw ratios. Examining the draw ratios of 52.90 (± 4.39), 66.47 (± 11.47), and 108.5 (± 19.57), the strength values stayed between 175 MPa to 200 MPa. This range of strengths is significantly greater than the 83.56 MPa (± 26.16 MPa) measured for the strands with a draw ratio of 9.521 (± 0.479). This demonstrates that it was necessary to reach draw ratios of at least 40 to maximize both the strength and modulus of the HX1000/PT 7067 composites. Moreover, adding HX1000 to PT 7067 consistently improved the strand strength, with all of the composite strands having tensile strengths greater than the value of 51.4 MPa (± 5.0 MPa) measured for the neat PT 7067 strands.

4.3.4 Uniaxially Compression Molded Composite Strands

To understand the effect that temperature would have on the TLCP fibrils in the composite strands when processed in a later step, several studies have been performed which consolidated composite strands into uniaxially reinforced composites [24, 47, 48]. It has been shown in previous work that the mechanical properties measured for individual strands were retained in uniaxially compression molded composites of PP/HX1000 [24], molded at 190°C, and PP/Vectra B950 [47], molded at 200°C. Meanwhile, uniaxially compression molded composites of polyamide 11/HX8000 [48] only retained about 67% of the original fiber modulus, with the reduction in stiffness being attributed to molecular relaxation of the HX8000 phase at the consolidation temperature of 195°C. Based on these previous results, it appears that consolidating the composite strands into uniaxial plaques was an effective method of determining how the high temperatures needed to melt the matrix polymer can affect the TLCP reinforcement.

To determine the effect of temperature on the HX1000 reinforcement, HX1000/PT 7067 (50/50 wt%) strands with a draw ratio of 66.47 (± 11.47) were consolidated at 260°C. After releasing the pressure needed for consolidation, some of these uniaxially reinforced composites were then kept at 260°C for an additional amount of time (up to one hour) to determine if the tensile modulus would decline over time. There was only a slight drop in stiffness due to consolidation; the individual strands had a tensile modulus of about 25.5 GPa while the uniaxial composites exhibited a slightly lower modulus of approximately 22 GPa (Figure 4.7). Furthermore, continued exposure to 260°C for up to one hour after consolidation did not cause the modulus to decline any further. This result indicates that any losses due to heat occurred initially during the consolidation step, with additional exposure to 260°C having no appreciable effect. However, it needs to be recognized that fiber misalignment and breakage during consolidation could also explain the reduction in modulus. Specifically, it was determined

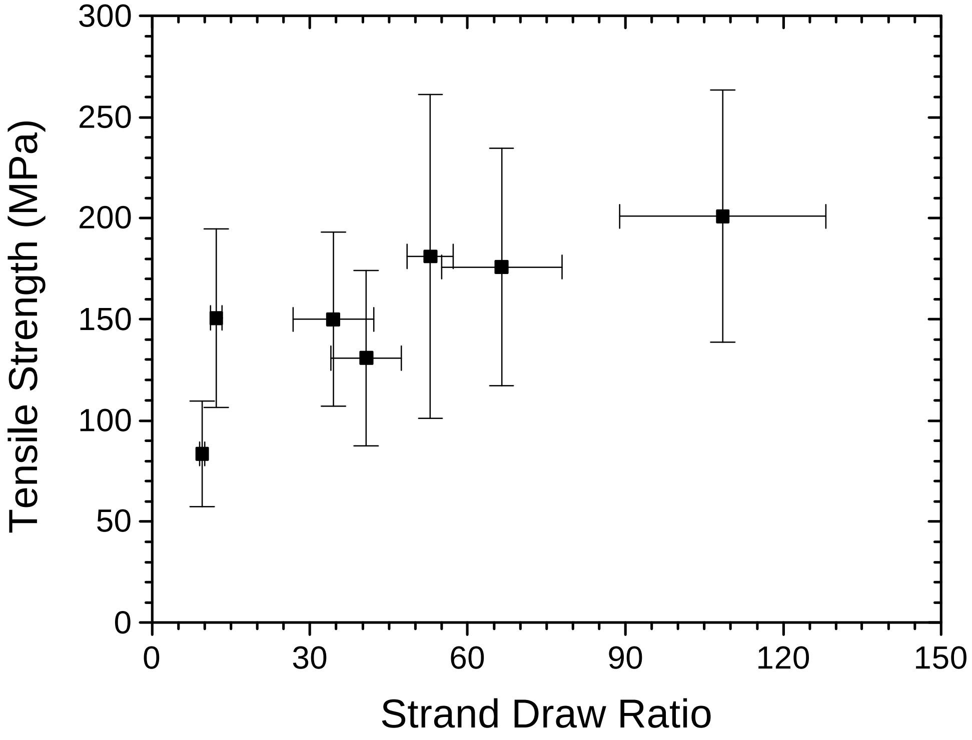

Figure 4.6: Tensile strength versus draw ratio for HX1000/PT 7067 (50/50 wt%) strands.

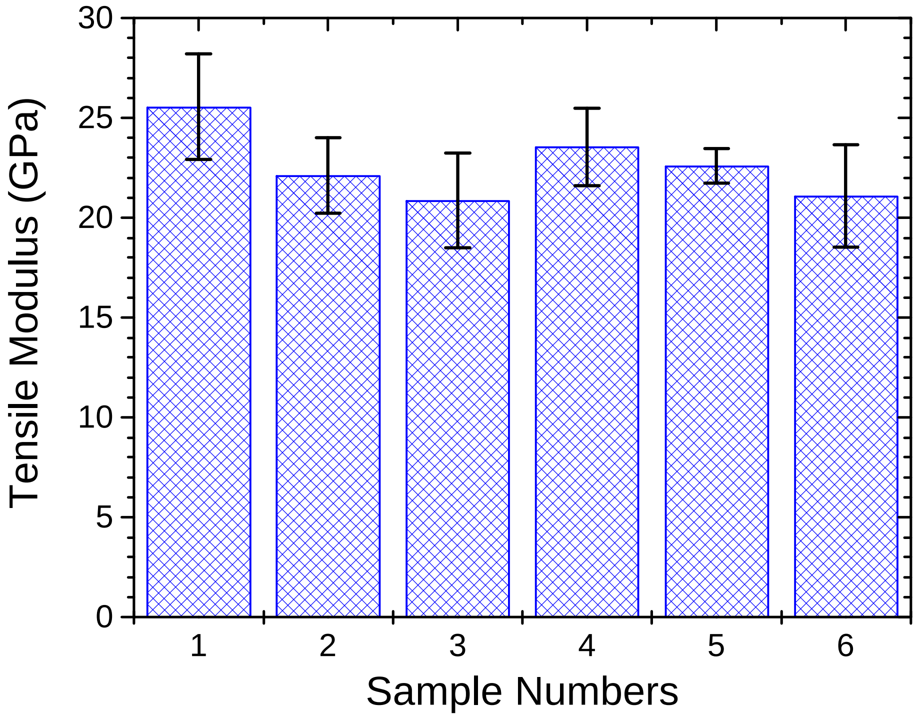

Figure 4.7: Tensile modulus of HX1000/PT 7067 (50/50 wt%) strands (draw ratio = 66.47 ± 11.47) before and after consolidation at 260°C, with the time the strands were exposed to 260°C beyond that needed for consolidation denoted. (1) = individual strands, (2) = consolidated strands, (3) consolidation + 5 min., (4) consolidation + 15 min., (5) consolidation + 30 min., and (6) consolidation + 60 min.

that fiber misalignment in the uniaxial composites accounted for a loss in modulus of 0.5 GPa [49]. Therefore, the behavior of the consolidated strands shows that most of the reinforcing potential of the HX1000 fibrils was retained when they were exposed to a temperature of 260°C and either there was an initial loss of modulus probably due to relaxation of orientation or there was some fibril damage and misalignment during consolidation.

4.3.5 Injection Molded Pregenerated Microcomposite Properties

The next focus of this work was to determine the effect of the matrix viscosity on the ability to maintain the reinforcing potential of the HX1000 fibrils during injection molding. In particular, the effect of diluting the strands containing 50 wt% TLCP with a lower viscosity PET, Rynite, versus the higher viscosity PET, PT 7067, was investigated. Two sets of composites were produced containing 20 wt% HX1000 fibrils. The first set was produced from HX1000/PT 7067 (20/80 wt%) composite strands, which were spun to a draw ratio of 48.12 (± 4.42), chopped, and injection molded. The second set was made with HX1000/PT 7067 (50/50 wt%) composite strands, which were spun to a draw ratio of 52.90 (± 4.90), chopped, dry blended with Rynite, and injection molded to produce composites with a composition of HX1000/PT 7067/Rynite (20/20/60 wt%). Note that within the standard deviations, the draw ratios of the two composite strands are equivalent, so any influence on mechanical properties that could exist due to draw is insignificant.

After injection molding the two sets of pregenerated microcomposites, the tensile and flexural properties were measured and compared. The tensile moduli for the HX1000/PT 7067/Rynite (20/20/60 wt%) composites were 4.586 GPa (± 0.192 GPa) in the machine direction and 3.304 GPa (± 0.230 GPa) in the transverse direction, versus just 3.106 GPa (± 0.146 GPa) in the machine direction and 3.086 GPa (± 0.241 GPa) in the transverse direction for the HX1000/PT 7067 (20/80 wt%) composites. Likewise, the flexural moduli for the HX1000/PT 7067/Rynite (20/20/60 wt%) composites were 5.176 GPa (± 0.310 GPa) in the machine direction and 3.635 GPa (± 0.233 GPa) in the transverse direction, compared to 4.281 GPa (± 0.102 GPa) and 4.099 GPa (± 0.433 GPa), respectively, for the HX1000/PT 7067 (20/80 wt%) composites. Based on the higher modulus of the HX1000/PT 7067/Rynite composites, it appears that adding a lower viscosity resin was helpful in preserving the reinforcing potential of the pregenerated HX1000 fibrils. In particular, it is believed that because the complex viscosity of Rynite was considerably lower than that of PT 7067 (Figure 4.8), less shear stress was applied to the HX1000 fibrils during plastication in the injection molder screw, which probably reduced the amount they were damaged. Also, it should be noted that in situ composites made with a composition of HX1000/PT 7067/Rynite (20/20/60 wt%) had lower tensile moduli than the pregenerated microcomposites [49]. For the in situ composites, the machine direction tensile modulus was 3.424 GPa (± 0.445 GPa) while

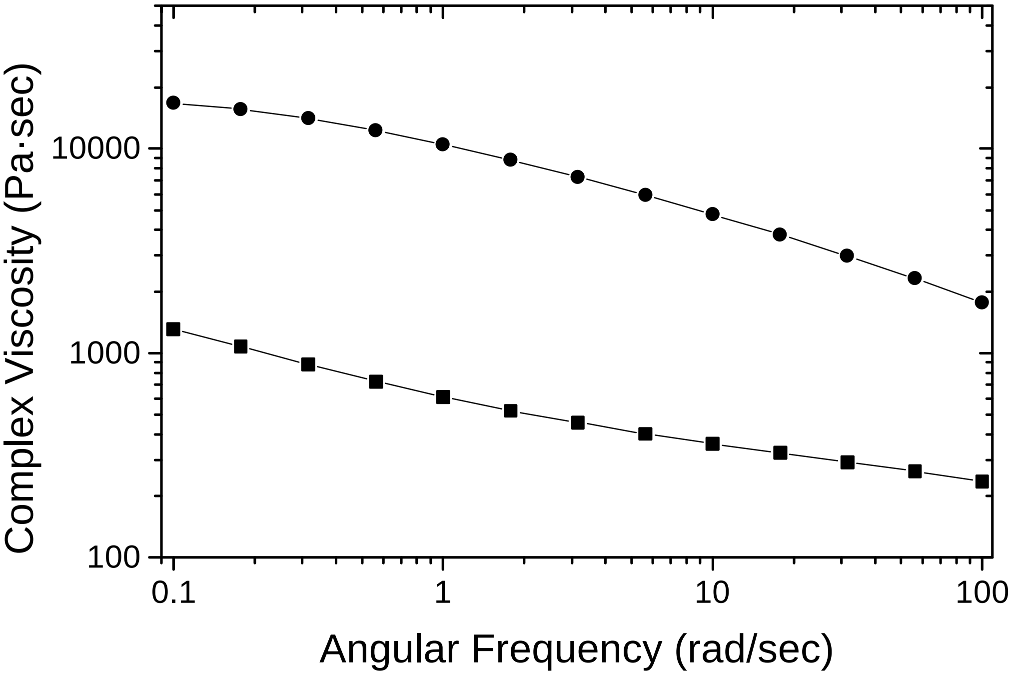

Figure 4.8: The complex viscosity (|η*|) versus angular frequency of the matrix polymers at 270°C. (■) = Rynite and (●) = PT 7067.

Table 4.2: The Effect of Composite Strand Draw Ratio on the Mechanical Properties of Pregenerated Microcomposites

Composition: HX1000/PT 7067/Rynite (30/30/40 wt%)

	Tensile Properties		**Flexural Properties**	
Draw Ratio = 9.521 (0.479)				
	Machine Direction	Transverse Direction	Machine Direction	Transverse Direction
Modulus (GPa)	4.800 (0.217)	3.122 (0.348)	5.399 (0.421)	3.845 (0.311)
Strength (MPa)	45.21 (10.09)	29.10 (4.801)	77.18 (3.890)	67.62 (3.996)
% Elongation	1.009 (0.228)	0.978 (0.122)		
Toughness (MPa)	0.253 (0.111)	0.148 (0.038)		
Draw Ratio = 40.67 (6.71)				
	Machine Direction	Transverse Direction	Machine Direction	Transverse Direction
Modulus (GPa)	5.161 (0.337)	3.310 (0.252)	4.453 (0.211)	3.837 (0.220)
Strength (MPa)	57.73 (8.788)	31.10 (5.345)	76.32 (3.682)	76.32 (5.743)
% Elongation	1.290 (0.226)	1.063 (0.246)		
Toughness (MPa)	0.346 (0.104)	0.142 (0.052)		
Draw Ratio = 52.90 (4.39)				
	Machine Direction	Transverse Direction	Machine Direction	Transverse Direction
Modulus (GPa)	5.593 (0.704)	4.010 (0.217)	6.200 (0.366)	3.711 (0.262)
Strength (MPa)	60.86 (8.825)	38.46 (4.323)	83.99 (3.353)	67.77 (5.619)
% Elongation	1.264 (0.147)	1.130 (0.116)		
Toughness (MPa)	0.386 (0.086)	0.203 (0.052)		
Draw Ratio = 66.47 (11.47)				
	Machine Direction	Transverse Direction	Machine Direction	Transverse Direction
Modulus (GPa)	5.162 (0.323)	3.230 (0.351)	5.556 (0.457)	3.641 (0.515)
Strength (MPa)	48.92 (7.660)	31.03 (6.278)	79.13 (2.986)	61.55 (7.535)
% Elongation	1.000 (0.151)	1.023 (0.183)		
Toughness (MPa)	0.255 (0.078)	0.168 (0.065)		
Draw Ratio = 108.5 (19.57)				
	Machine Direction	Transverse Direction	Machine Direction	Transverse Direction
Modulus (GPa)	5.727 (0.432)	3.362 (0.414)	6.038 (0.522)	4.216 (0.191)
Strength (MPa)	58.22 (7.814)	34.04 (7.539)	79.15 (7.212)	72.89 (4.827)
% Elongation	1.088 (0.100)	1.023 (0.183)		
Toughness (MPa)	0.330 (0.083)	0.193 (0.069)		

Note: Standard deviations given in parentheses.

transverse direction tensile modulus was 2.825 GPa (± 0.203 GPa). Thus, the results demonstrate that the pregenerated microcomposite is stiffer by almost 1.2 GPa in the machine direction and 0.5 GPa in the transverse direction.

The effect of strand draw ratio on the final mechanical properties of injection molded pregenerated microcomposites was also examined. To do this, HX1000/PT 7067 (50/50 wt%) strands were spun with several different draw ratios. These draw ratios ranged from 9.521 (± 0.479) to 108.5 (± 19.57), with three draw ratios in excess of 50. As shown in Table 4.2, composites produced using the lowest draw ratio also had the lowest moduli but, unlike the results reported by Handlos and Baird [25], the differences in the moduli were generally within the standard deviations of the tests. For example, using strands with a draw ratio of 9.521 (± 0.479) yielded a machine direction flexural modulus of 5.399 GPa (± 0.421 GPa). Meanwhile, when strands with a draw ratio of 108.5 (± 19.57) were used, the flexural modulus only increased to 6.038 GPa (± 0.522 GPa), showing that no effect due to fiber draw ratio is discernible within the experimental error. Additionally, the effect of draw ratio was usually not statistically significant for the other mechanical properties, although the composites produced using the strands with the lowest draw ratio typically had the lowest properties. Thus, although the results suggest that it is necessary to have composite strands with a draw ratio of at least 40 to maximize mechanical properties, draw ratios as low as 9.5 still yield properties which are barely statistically different from those obtained using strands with a draw ratio of 108.5.

There were several reasons why it was difficult to establish a significant relationship between draw ratio and the pregenerated microcomposite tensile modulus. The first reason was that the low draw ratio strands also had high moduli. The strands with a draw ratio of 9.521 (± 0.479) had a tensile modulus of 19.88 GPa (± 1.30 GPa), versus 26.76 GPa (± 3.22 GPa) for composite strands with a draw ratio of 108.5 (± 19.57). Although this is a statistically significant difference in stiffness, it is significant by only 2.36 GPa. Second, the pregenerated microcomposites contained only up to 30 wt% HX1000 and the fibrils were distributed in the plaque in a random fashion, so the differences in the moduli due to draw ratio would be smaller. Third, the pregenerated microcomposites did not meet the level of reinforcement expected from composite theory, lowering the modulus of the pregenerated microcomposites and helping mask any effects due to draw ratio. For these reasons, it was clear that it would be difficult to detect significant differences in the moduli of the pregenerated microcomposites over the range of draw ratios tested.

4.3.6 Comparison to Theory and Glass Reinforced PET

Before comparing the properties of the microcomposites to those of glass-reinforced PET, the theoretically predicted modulus values were calculated and compared. For these calculations, a density of 2.59 g/cm^3 and a modulus of 69 GPa was used for the glass fiber, while a density of 1.25 g/cm^3 and a modulus of 49.86 GPa was used for the HX1000 fibrils. Using the Tsai-Halpin equation and assuming a planar isotropic distribution of fibers, the pregenerated microcomposites were predicted to have moduli of 4.15 GPa at 10 wt% HX1000, 5.84 GPa at 20 wt% HX1000, and 7.49 GPa at 30 wt% HX1000. These values are slightly greater than those calculated for the glass filled PET, with the predicted moduli being 3.54 GPa with 10 wt% glass fiber, 5.07 GPa with 20 wt% glass fiber, and 6.80 GPa with 30 wt% glass fiber. The reason the theoretical modulus values for the HX1000 filled PET are higher is due to the fact that although the HX1000 has a lower modulus than glass fiber (50 GPa versus 69 GPa), it also has a much lower density of 1.25 g/cm^3, versus 2.59 g/cm^3 ascribed to E-glass fiber. Therefore, because the Tsai-Halpin equation is based on volume fractions, the lower tensile modulus of HX1000 is offset by the fact that the HX1000 fibrils occupy a larger volume fraction of the composite than glass fiber at the same weight fraction of loading.

Comparing the experimental tensile and flexural moduli of the pregenerated microcomposites (Table 4.2) to those of the glass-fiber reinforced PET (Table 4.1) showed that higher moduli were achieved with glass fiber reinforcement. This was the case despite the fact that theoretically, if the full reinforcing potential of both fibers was realized, the HX1000 reinforced composites would have slightly higher moduli. Examining the machine direction modulus at 30 wt% loading serves to illustrate the difference in reinforcement. At 30 wt% glass fiber, a machine direction tensile modulus of 9.209 GPa was achieved versus just 5.727 GPa for the pregenerated microcomposite. Hence, although significant reinforcement by the pregenerated HX1000 fibrils was obtained, the level of reinforcement still fell short of the theoretically expected values and what was accomplished using the same weight fraction of glass fiber.

The difference between the glass fiber and HX1000 fibril reinforcement emphasizes that although theoretically the HX1000 reinforced composites should be slightly stiffer, the injection molding step does not have the same affect on glass fiber as it does on HX1000 fibrils. In particular, the HX1000 fibrils appear to be more sensitive to shear and thermal history, making it difficult to achieve the theoretically expected levels of reinforcement. One key reason for the difference between the two forms of reinforcement lies in the fact that the injection molding temperatures exceed the glass transition temperature of the TLCP. This means that rather than the HX1000 being in a glassy state, it is in a rubbery state, making it less resistant to the forces encountered in the injection molding step. Morphologically, this is evident in the twisted and bent shapes of some of the HX1000 fibrils after the injection molding step (as shown in Figure 4.9).

In addition to having higher moduli, the glass fiber reinforced PET also consistently outperformed the pregenerated microcomposite in the categories of strength,

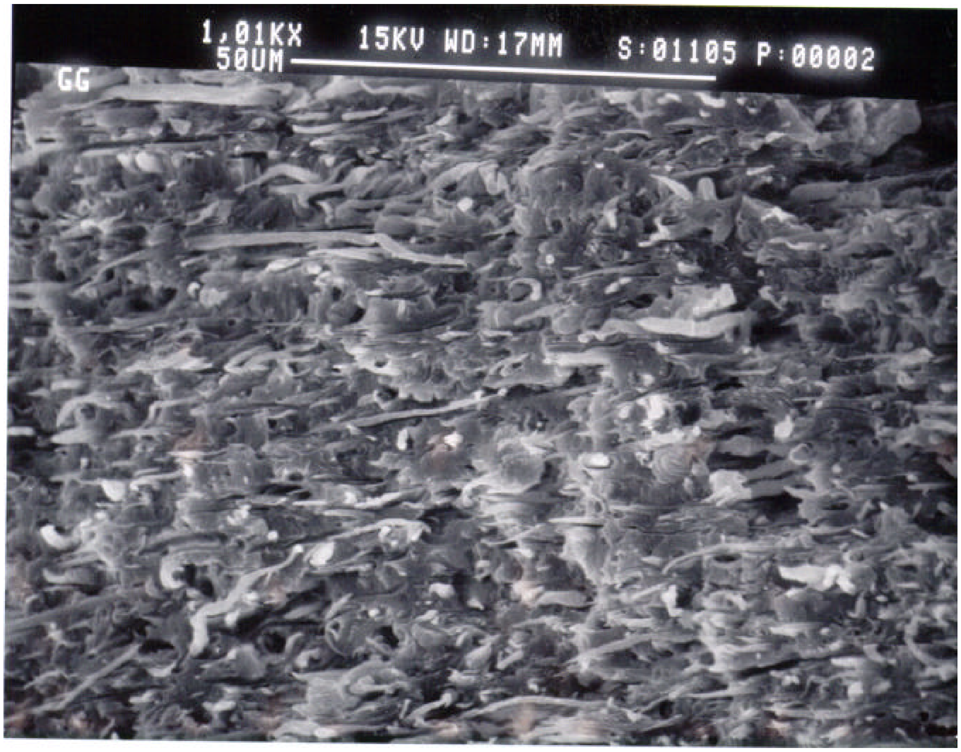

Figure 4.9: Scanning electron micrograph of HX1000 fibrils in an injection molded pregenerated microcomposite.

percent elongation, and toughness. However, a few key points need to be recognized in this comparison. First, the glass fiber had a sizing agent on its surface while the HX1000 fibrils were not sized. This distinction is important because sizing agents are used to obtain good adhesion between the fiber and matrix. This means that because the HX1000 fibrils were not sized, the adhesion between the matrix and reinforcement was less than optimal, which might have accounted for the lower properties. However, it has been shown that it is possible to improve the adhesion in TLCP reinforced thermoplastics by using reactive components [50 - 52]. Therefore, higher strengths, percent elongations, and toughnesses should be possible by using a small amount of a reactive component in the injection molding step.

A second reason that the HX1000 fibril filled composites had lower mechanical properties than the glass filled composites was because HX1000 was not as strong as glass. The strength of glass fiber has been cited as ranging from 1.72 GPa to over 2.07 GPa [10, 11]. Meanwhile, neat HX1000 only had a strength of about 300 MPa. Based on the difference in strength between the two neat materials, it is not surprising that composites containing 30 wt% glass fiber are one and a half times as strong as those reinforced with HX1000 fibrils. Still, it needs to be remembered that the interfacial adhesion between the HX1000 fibrils and the matrix has not been addressed. This means that despite the disparity in tensile strengths between neat glass fiber and HX1000 strands, improved adhesion between the matrix and the TLCP could yield strengths which are competitive with glass filled materials. Also, it should be noted that other TLCPs have higher strengths and moduli, so using this processing scheme with these materials offers a method of obtaining mechanical properties more competitive with glass fiber reinforcement.

Along with tensile and flexural properties, the dynamic mechanical properties and surface roughnesses of the pregenerated microcomposites were compared to glass-filled PET. Specifically, the dynamic mechanical thermal analysis was performed to show how exposing the pregenerated microcomposites to elevated temperatures would affect the stiffness of the material (a form of heat distortion behavior). Surface profilometry was used to determine if smaller fibril size would lead to composites with smoother surfaces. Figure 4.10 illustrates the size difference between the glass fibers and HX1000 fibrils, with the diameters of the glass fibers being approximately 12 μm, while the HX1000 fibrils possessing diameters around 2 μm. With some of the fibers located at or close to the sample surface, the larger diameters of the glass fibers can produce a rougher surface than TLCP fibrils [53].

For the dynamic mechanical thermal analysis, tests were run on neat Rynite, Rynite 530, and a pregenerated microcomposite composed of HX1000/PT 7067/Rynite (30/30/40 wt%). It should be noted that the strands used in producing the pregenerated microcomposite had a draw ratio of 52.90 (± 4.39), so the reinforcing potential of the

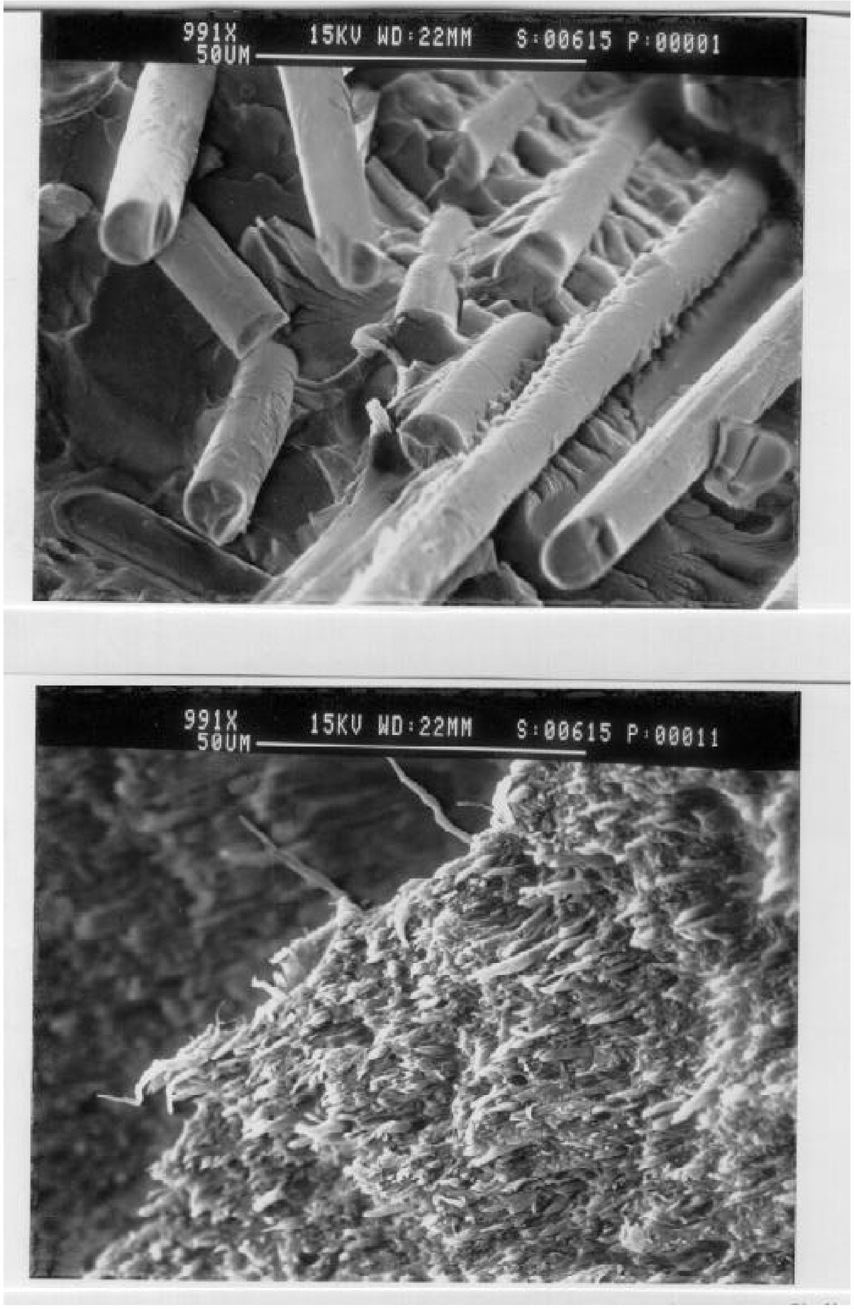

Figure 4.10: Scanning electron micrographs comparing the size of HX1000 fibrils to glass fiber. Top: Glass fiber in Rynite 530 and Bottom: HX1000 fibrils in HX1000/PT 7067/Rynite (30/30/40 wt%).

HX1000 phase was maximized. The storage moduli of neat Rynite, glass-fiber reinforced PET, and the pregenerated microcomposites were measured with respect to temperature as the samples were heated at a rate of 2.5°C/min. The pregenerated microcomposites showed behavior that was comparable to glass filled PET up to approximately 150°C, with both specimens possessing storage moduli greater than that of neat Rynite (Figure 4.11). Yet, once the sample temperature reached 150°C, the storage modulus of the pregenerated microcomposite began to drop because the HX1000 began to lose its stiffness. In particular, the storage modulus of the pregenerated microcomposite approached that of neat PET once the temperature reached 220°C. From this it can be concluded that for temperatures of 150°C or less, the HX1000 fibrils provide approximately the same level of stiffness as the glass fibers.

To determine how the surface roughness was affected by the type of reinforcement and loading level, tests were conducted on neat PET as well as specimens containing 10, 20, and 30 wt% reinforcement. These tests were performed on both pregenerated microcomposites, made with strands having a draw ratio of 108.5 (± 19.57), as well as glass-fiber filled PET. Examining the data, only at a loading level of 30 wt% reinforcement could an appreciable difference between glass fiber reinforcement and HX1000 fibril reinforcement be discerned (as presented in Table 4.3). Namely, at 30 wt% reinforcement, the pregenerated microcomposite only had an average surface roughness of 0.2537 μm, while the glass-filled PET had a roughness of 1.342 μm. The sudden increase in surface roughness at a loading of 30 wt% glass fiber could be related to two factors: 1) the volume fraction of glass fiber present and 2) the size of the reinforcement. At a loading of 30 wt%, 18.4 volume percent (vol%) of the plaque was taken up by glass fiber. At this level of reinforcement, it appears that enough of the 12 μm diameter glass fibers were placed at the sample surface to significantly affect the surface roughness (Figure 4.12). Meanwhile, even though a loading level of 30 wt% HX1000 meant that 31.6 vol% of the plaque was occupied by the TLCP fibrils, the higher volume fraction appears to have been offset the smaller size of the fibrils. Because the HX1000 fibrils had diameters of around 2 μm, it appears likely that they protruded a shorter distance from the surface of the plaque, yielding a smoother surface.

4.4 Conclusions

Three TLCPs and one TLCP/TLCP blend were evaluated for the pregenerated microcomposite process, from which HX1000 was chosen as the TLCP to use. This choice was based on its ability to be cooled to well under 300°C, the retention of stiffness after being heated to 260°C for one minute, the glass transition temperature of 160°C, and the absence of any melting endotherms. These characteristics allowed the TLCP to be spun into composite strands and be chopped and injection molded while still retaining some of its reinforcing potential.

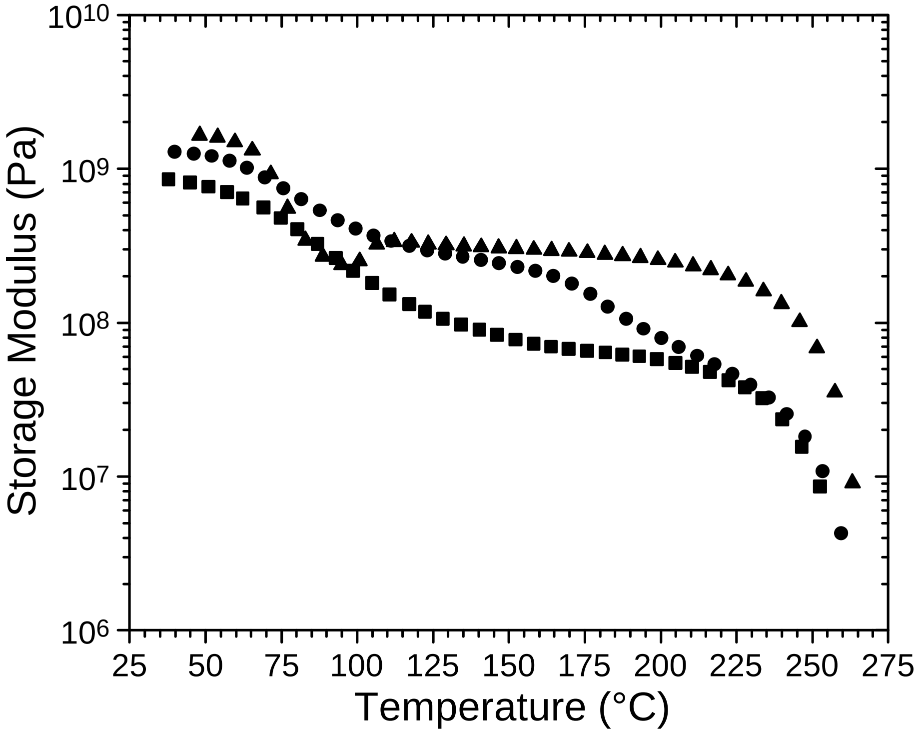

Figure 4.11: Storage modulus (G') versus temperature for Rynite = (■), HX1000/PT 7067/Rynite (30/30/40 wt%) pregenerated microcomposite = (●), and Rynite 530 = (▲) using a heating rate of 2.5°C/min.

Table 4.3: Arithmetic Average Surface Roughnesses of Glass and HX1000 Filled PET Composites

Weight % Reinforcement [vol% glass fiber / vol% HX1000 fibril][a]	Surface Roughness of Glass Filled PET (μm)	Surface Roughness of HX1000 Fibril Filled PET (μm)
0 [0 / 0]	0.031 (0.014)	0.031 (0.014)
10 [5.43 / 10.76]	0.180 (0.082)	0.206 (0.088)
20 [11.51 / 21.29]	0.312 (0.119)	0.321 (0.089)
30 [18.37 / 31.59]	1.342 (0.329)	0.254 (0.115)

Note: Standard deviations given in parentheses.

[a] The numbers in brackets are the volume percentages of each reinforcing material at the given weight fraction, with the glass fiber volume percent first and the HX1000 volume percent second.

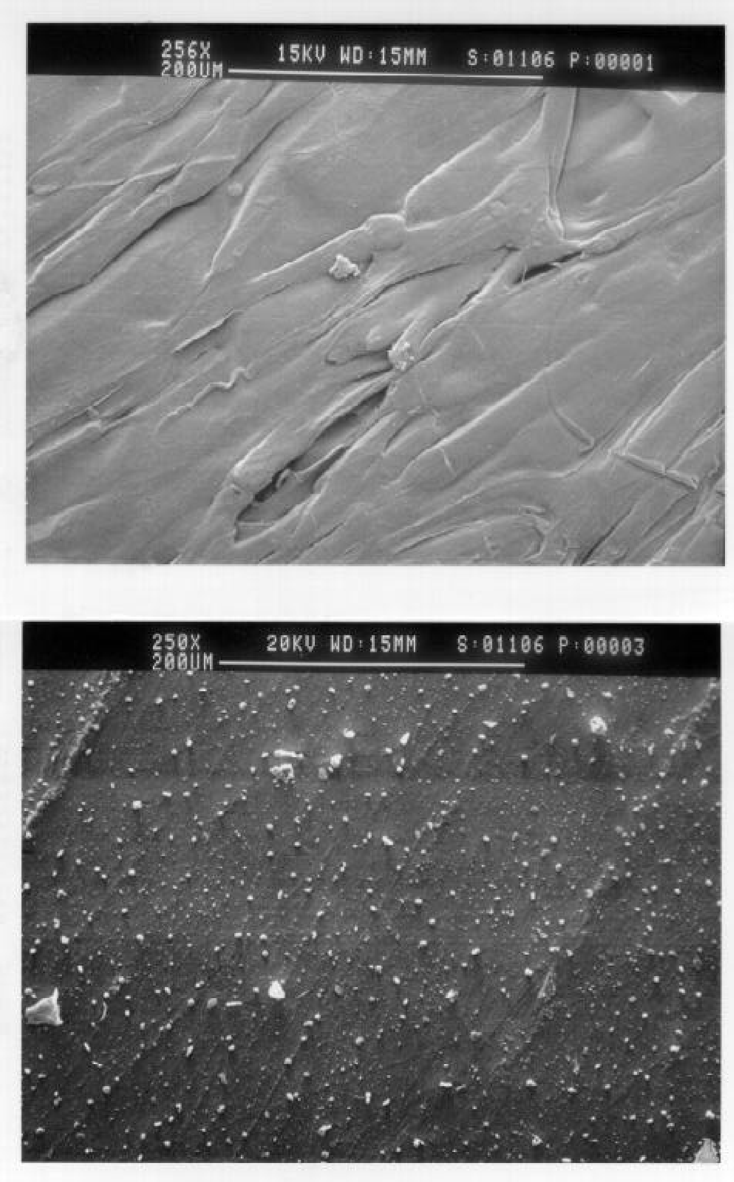

Figure 4.12: Scanning electron micrographs of the surfaces of the composite plaques. Top: Glass fiber in Rynite 530 and Bottom: HX1000 fibrils in HX1000/PT 7067/Rynite (30/30/40 wt%).

It was determined that higher pregenerated microcomposite moduli were obtained by diluting chopped composite strands with a low viscosity resin (Rynite). Specifically, by dry blending the composite strands with Rynite, which was less viscous than PT 7067 by an order of magnitude, the TLCP fibrils were subjected to lower shear stresses during injection molding. In turn, it is believed that this reduced the degree of damage they sustained in the injection molding step, allowing the HX1000 fibrils to retain their reinforcing potential.

It was not possible to show a statistically significant relationship between composite strand draw ratio and pregenerated microcomposite mechanical properties. This was attributed to two main factors: 1) the increase in modulus as the draw ratio increased from 9.5 to 108.5 was not great and 2) the effect of draw ratio on the tensile modulus was masked by dilution and randomly distributing the reinforcement in the plaque.

When compared to the neat PET, the pregenerated microcomposites had significantly better mechanical properties. In particular, the moduli of the pregenerated microcomposites were as high as 2.5 times that of the neat resins, proving that the pregenerated microcomposite process was a viable method of reinforcing commodity resins. Meanwhile, comparing the pregenerated microcomposites to glass filled PET showed that glass fiber provided more reinforcement than the HX1000 fibrils, but the pregenerated microcomposites had similar dynamic mechanical properties up to 150°C and smoother surfaces. These results serve to further emphasize that if the theoretically expected levels of stiffness are achieved, these composites have other characteristics which would make them desirable substitutes to other composite materials, such as glass fiber filled resins. To improve on the mechanical properties, it may be necessary to use a matrix with lower processing temperatures, a TLCP with a higher glass transition temperature, and a TLCP with a higher tensile strength and modulus.

4.5 Acknowledgments

The authors would like to gratefully recognize the support from the Army Research Office (Grant No. DAAH04-94-G-0282). We also offer our appreciation to DuPont for donating the PET and TLCPs used in this study. In addition, we would like to thank Dr. Eiss for the surface profilometry work and Dr. Wilkes for the use of the scanning electron microscope.

4.6 References

---

1 A. Sigmann, A. Dagan, and S. Kenig, *Polymer*, 26, 1325 (1984).

2 R.A. Weiss, W. Huh, and L. Nicolais, *Polym. Eng. Sci.*, 27 (9), 684 (1987).

3 G. Kiss, *Polym. Eng. Sci.*, 27, 410 (1987).

4 A.I. Isayev and M. Modic, *Polym. Comp.*, 8, 158 (1987).

5 K.G. Blizard and D.G. Baird, *Polym. Eng. Sci.*, 27 (9), 653 (1987).

6 D. Acierno and M.R. Nobile, in *Thermotropic Liquid Crystal Polymer Blends (Chap. 3)*,ed. F.P La Mantia Technomic Publ. Co, Lancaster PA 1993.

7 G.D. Figuly, in *Polymeric Materials Encyclopedia (Liquid Crystalline Polymers (Thermotropic Polyesters))*, ed. J.C. Salamone, CRC Press, Boca Raton FL 1996.

8 H.N. Yoon, L.F. Charbonneau, and G.W. Calundann, *Adv. Mat'ls*, 4 (3), 206 (1992).

9 S. Kessler, in *Plastics Additives and Modifiers Handbook (Chap. 48)*, ed. J. Edenbaum, Van Nostrand Reinhold, New York 1992.

10 P.K. Mallick, *Fiber-Reinforced Composites*, Marcel Dekker, New York 1988.

11 PPG Industries, Inc., in *Modern Platics Encyclopedia '92*, McGraw-Hill, New York 1992.

12 W.R. Graner, in *Handbook of Composites*, Ed. G. Lubin, Van Nostrand Reinhold, New York 1982.

13 A.A. Handlos and D.G. Baird, *J. Macromol. Sci., Rev. Macromol. Chem. Phys.*, C35, 183 (1995).

14 A. Datta, H.H. Chen, and D.G. Baird, *Polymer,* 34 (4), 759 (1993).

15 J.C. Halpin and J.L. Kardos, *Polym. Eng. Sci.*, 16, 344 (1976).

16 E.A. Sabol, Master’s Thesis, Virginia Polytechnic Institute and State University, Blacksburg VA 1994.

17 M.S. Silverstein, A. Hiltner, and E. Baer, *J. Appl. Polym. Sci.*, 43, 157 (1991).

18 F.P. La Mantia, G. Titomanlio, and A. Valenza, in *Thermotropic Liquid Crystalline Polymer Blends (Chap. 5)*, ed. F.P. La Mantia, Technomic, Lancaster PA 1993.

19 S.S. Bafna, J.P. de Souza, T. Sun, and D.G. Baird, *Polym. Eng. Sci.*, 33 (13), 808 (1993).

20 H.J. O’Donnell, PhD Dissertation, Virginia Polytechnic Institute and State University, Blacksburg (VA), 1994.

21 H.J. O’Donnell and D.G. Baird, *Polym. Eng. Sci.*, 36 (7), 963 (1996).

22 H.J. O’Donnell and D.G. Baird, *Int’l Polym. Proc.*, XI (3), (1996).

23 M.T. Heino, T.P. Vainio, and J.V. Seppälä, *Polym. & Polym. Comp.,* 1 (6), 439 (1993).

24 E.A. Sabol, A.A. Handlos, and D.G. Baird, *Polym. Compos.*, 16 (4), 330 (1995).

25 A.A. Handlos and D.G. Baird, *Int'l Polym. Proc.*, XI (1), 1-13 (1996).

26 A.A. Handlos, PhD Dissertation, Virginia Polytechnic Institute and State University, Blacksburg (VA) 1994.

27 D.G. Baird and A.M. Sukhadia, *U.S. Patent 5,225,488* (1993).

---

28 A.M. Sukhadia, A. Datta, and D.G. Baird, *Int’l Polym. Proc.*, VII (3), 218 (1992).

29 P. Magagnini, in *Thermotropic Liquid Crystalline Polymer Blends (Chap. 1)*, ed. by F.P. La Mantia, Technomic, Lancaster, PA 1993.

30 P. Avakian, J.C. Coburn, M.S. Connolly, and B.B. Sauer, *Polymer*, 37 (17), 3843 (1996).

31 J.J. Kleinschuster (DuPont), *U.S. Patent 3,991,014* (1976).

32 R.S. Irwin (DuPont), *U.S. Patent 4,487,916* (1984).

33 R.S. Irwin (DuPont), *U.S. Patent 4,496,712* (1985).

34 R.S. Irwin (DuPont), *U.S. Patent 4,499,259* (1985).

35 M.S. Connolly (DuPont), *U.S. Patent 4,664,972* (1987).

36 M.R. Samuels and M.G. Waggoner (DuPont), *U.S. Patent 5,466,773* (1995).

37 M.R. Samuels and M.G. Waggoner (DuPont), *U.S. Patent 5,525,700* (1996).

38 DuPont Product Information, *Typical Properties of Selar$^{(R)}$ PT*, Technology Bulletin H-37071.

39 E.A. Sabol and D.G. Baird, *Int'l Polym. Proc.*, X (2), 124 (1995).

40 Y.G. Lin and H.H. Winter, *Macromolecules*, 24 (10), 2877 (1991).

41 Y.G. Lin and H.H. Winter, *Macromolecules*, 21, 2439 (1988).

42 H. Muramatsu and W.R. Krigbaum, *J. Polym. Sci.: Part B: Polym. Phys.*, 25, 2303 (1987).

43 W.R. Krigbaum, C.K. Liu, and D.-K. Yang, *J. Polym. Sci.: Part B: Polym. Phys.*, 26, 1711 (1988).

44 H.J. O’Donnell and D.G. Baird, *Polym. Eng. Sci.*, 36 (7), 963 (1996).

45 C.S. Brown and P.T. Alder, in *Polymer Blends and Alloys (Chap. 8)*, ed. M.J. Folkes and P.S. Hope, Chapman and Hall, London UK 1993.

46 L.A. Utracki and T. Vu Khanh, in *Multicomponent Polymer Systems*, ed. I.S. Miles, John Wiley and Sons, New York 1992.

47 C.G. Robertson, J.P. de Souza, and D.G. Baird, in *Liquid-Crystalline Polymer Systems: Technological Advances (Chap. 6 - ACS Symposium Series 632)*, ed. A.I. Isayev, T. Kyu, and S.Z.D. Cheng, American Chemical Society 1996.

48 R.K. Krishnaswamy and D.G. Baird, *Polym. Compos.*, 18 (4), 526 (1997).

49 M.A. McLeod, PhD Dissertation, Virginia Polytechnic Institute and State Univerity (1997).

50 M.T. Heino and J.V. Seppälä, *J. Appl. Polym. Sci.*, 48 (9), 1677 (1993).

51 H.J. O'Donnell and D.G. Baird, *Polymer*, 36 (16), 3113 (1995).

52 A. Datta and D.G. Baird, *Polymer*, 36 (3), 505 (1995).

53 S.G. Advani, in *International Encyclopedia of Composites (Vol. 3)*, ed. S.M. Lee, VCH, New York 1990.